

Highly Nonlinear and Low Confinement Loss Photonic Crystal Fiber Using GaP Slot Core

Md Borhan Mia, Animesh Bala, Kanan Roy Chowdhury and Mohammad Faisal

Abstract— This paper presents a triangular lattice photonic crystal fiber with very high nonlinear coefficient. Finite element method (FEM) is used to scrutinize different optical properties of proposed highly nonlinear photonic crystal fiber (HNL-PCF). The HNL-PCF exhibits a high nonlinearity up to $10 \times 10^4 \text{ W}^{-1} \text{ km}^{-1}$ over the wavelength of 1500 nm to 1700 nm. Moreover, proposed HNL-PCF shows a very low confinement loss of 10^{-3} dB/km at 1550 nm wavelength. Furthermore, chromatic dispersion, dispersion slope, effective area etc. are also analyzed thoroughly. The proposed fiber will be a suitable candidate for broadband dispersion compensation, sensor devices and supercontinuum generation.

Index terms—Finite element method, nonlinear coefficient, photonic crystal fiber, and birefringence.

I. INTRODUCTION

Photonic crystal fibers or microstructure holey fibers exhibit diversified properties which furnishes some new applications such as supercontinuum generation, fiber sensors and lasers. High nonlinearity is one of the indispensable properties of photonic crystal fibers for many practical applications including supercontinuum generation, optical parameter amplification, optical wavelength conversion [1], [2]. Compared to standard single mode fibers (SMFs), PCFs have many tunable properties, i.e.; air hole diameter, pitch, cladding, background material, doped core. These flexibility provides better control over dispersion slope, nonlinearity, birefringence, confinement loss etc.; in PCF which were unattainable in SMFs. PCFs are classified into two group, index guiding PCF and photonic band gap (PBG) guiding PCFs. In both PCFs, high refractive index contrast is maintained between core and cladding.

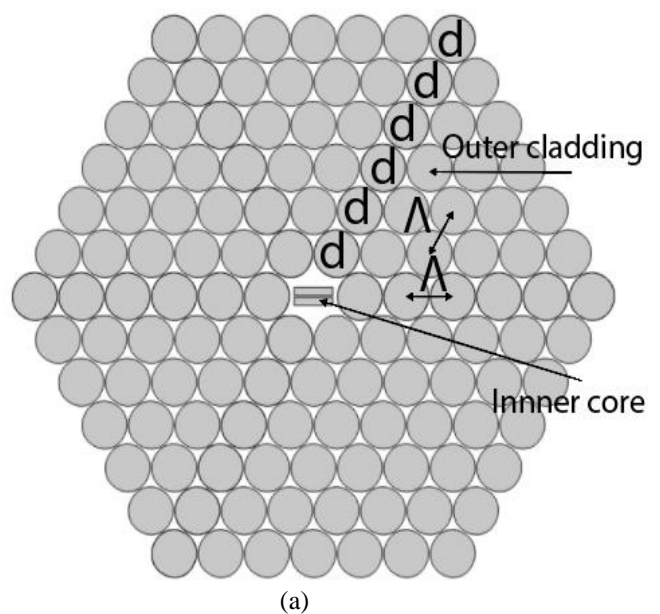
To attain the high nonlinearity researchers have studied the behavior of PCFs by using nanostructure of high refractive index in the core region. Nonlinear coefficient in pure silica core PCFs is only in the range of $100 \text{ W}^{-1} \text{ km}^{-1}$ because of nonlinear refractive index of pure silica is about $29.6 \times 10^{-21} \text{ m}^2/\text{W}$. Therefore, higher refractive index materials are used in the core to improve nonlinearity. Recently, Liao et al. [3] proposed a highly nonlinear PCF using nano scale slot core. The PCF exhibits a very high nonlinearity up to $3.5739 \times 10^4 \text{ W}^{-1} \text{ km}^{-1}$. However, confinement loss issue is ignored. Huang et al. proposed a slot spiral silicon photonic crystal fiber having a high nonlinear coefficient up to $1068 \text{ W}^{-1} \text{ m}^{-1}$ [4]. Li and Zhao used gold nano wires in the core region and attained boosted polarization dependent coupling and transmission [5]. Liao et al. [6] proposed a highly nonlinear spiral photonic crystal fiber exhibiting nonlinear coefficient of $226 \text{ W}^{-1} \text{ m}^{-1}$ at the communication band. Amin et al. [7] proposed a spiral high nonlinear photonic crystal fiber using GaP strips in the core. The fiber shows a high nonlinearity of $10^4 \text{ W}^{-1} \text{ km}^{-1}$.

Nevertheless, fiber exhibits confinement loss of 10^3 and 10^{-10} dB/km for x and y polarization mode, respectively at 1550 nm wavelength. To fabricate fibers with nanoscale slot core, recently some articles are realizable [8].

In this paper, a triangular lattice photonic crystal fiber is proposed which shows a very high nonlinearity up to $8 \times 10^4 \text{ W}^{-1} \text{ km}^{-1}$ at 1550 nm wavelength. It exhibits nonlinearity of 10×10^4 to $2 \times 10^4 \text{ W}^{-1} \text{ km}^{-1}$ from 1550 nm to 1770 nm wavelength range. In addition, it show a very low confinement loss of 10^{-3} dB/km at communication band. To our knowledge this is the best result compared to recently published articles. Moreover, HNL-PCF shows a very high dispersion up to $-9000 \text{ ps}/(\text{nm} \cdot \text{km})$ at 1550 nm wavelength. Therefore, design fiber can be useful supercontinuum generation, optical parameter amplification and broadband dispersion compensation.

II. FIBER DESIGN

The transverse cross section of the proposed HNL-PCF with magnified view of the slot core is demonstrated in Fig. 1. The design is kept as simple as possible. Six rings of air holes consist the cladding region. The air hole diameter in cladding region, $d = 0.58 \mu\text{m}$ with the pitch value of $\Lambda = 0.75 \mu\text{m}$. Air filling fraction in cladding profile is $d/\Lambda = 0.77$ which is fabrication feasible. Two identical rectangular GaP strips are introduced in the core with a slot of $L_s = 0.12 \mu\text{m}$. The length and width of the strips are $d_x = 0.58 \mu\text{m}$ and $d_y = 0.096 \mu\text{m}$, respectively. The amplified view of the core in Fig. 1(a) exhibits d_x , d_y and L_s . The background material is silica (SiO_2) which is industrially accessible.



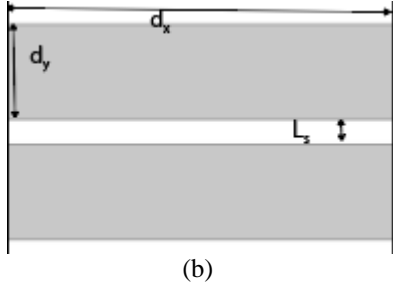


Fig. 1 (a) Transverse cross section of the proposed HNL-PCF (b) magnified view of core.

III. SIMULATION AND RESULT

A full vector Finite Element Method (FEM) is used to analyze different optical properties of the proposed design. COMSOL MULTIPHYSICS 5.0 is used to simulate the full design. Modal analysis has been studied by solving the eigen value problems drawn from Maxwell's equation. A perfectly matched layer (PML) is positioned at the outermost ring to prevent reflection [9]. Since refractive indices depend on wavelength, Sellmeier's constants for silica (SiO_2) and GaP are directly employed in simulation to improve the accuracy. Once modal refractive index, η_{eff} is obtained, other parameters like chromatic dispersion $D(\lambda)$, nonlinear coefficient γ , confinement loss L_c and effective area A_{eff} can be tailored from their equations.

$$\gamma = \frac{2\pi n_2}{\lambda A_{eff}} \quad (1)$$

$$A_{eff} = \frac{(\iint |E|^2 dx dy)^2}{\iint |E|^4 dx dy} \quad (2)$$

$$L_c = \frac{20 \times 10^6}{\ln(10)} k_0 \text{Im} |\eta_{eff}| \quad (3)$$

$$D(\lambda) = -\frac{\lambda}{c} \frac{d^2 \text{Re} |\eta_{eff}|}{d\lambda^2} \quad (4)$$

Where, $\text{Re} |\eta_{eff}|$ and $\text{Im} |\eta_{eff}|$ are the real and imaginary part of the effective refractive index, respectively; c is the velocity of light in vacuum, λ is the operating wavelength, E is the electric field vector, $k_0 = \frac{2\pi}{\lambda}$, is the wave number in free space; n_2 is the Kerr constant. For GaP, the $n_2 = 6.63 \times 10^{-18} \text{ m}^2 \text{W}^{-1}$ [10]. Three termed Sellmeier formula for silica (SiO_2) and GaP are directly included in simulation.

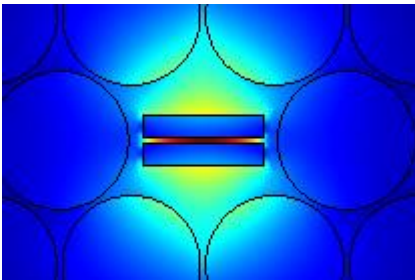


Fig. 2 Poynting vector profile of the proposed HNL-PCF.

Fundamental mode field distribution of the proposed fiber with parameters $\Lambda = 0.75 \mu\text{m}$, $d = 0.58 \mu\text{m}$, $d_x = 0.5 \mu\text{m}$, $d_y = 0.096 \mu\text{m}$ and $L_s = 0.12 \mu\text{m}$ is depicted in Fig. 2. It is apparent that fundamental mode is well confined in GaP slot region meaning small effective mode can be obtained from the proposed fiber. The effective mode of the proposed fiber as a function of wavelength is explained in Fig. 3. From Fig 3, it is seen that effective area at 1550 nm wavelength is $0.3 \mu\text{m}^2$, which is very small. This small area of the effective mode gives rise a huge nonlinearity.

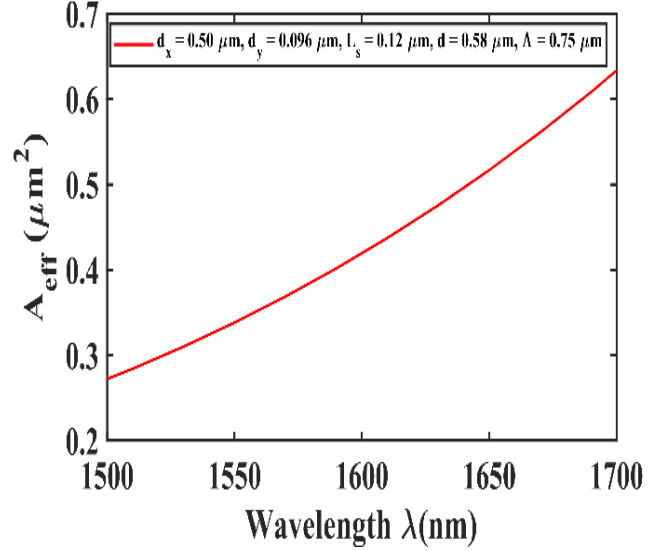
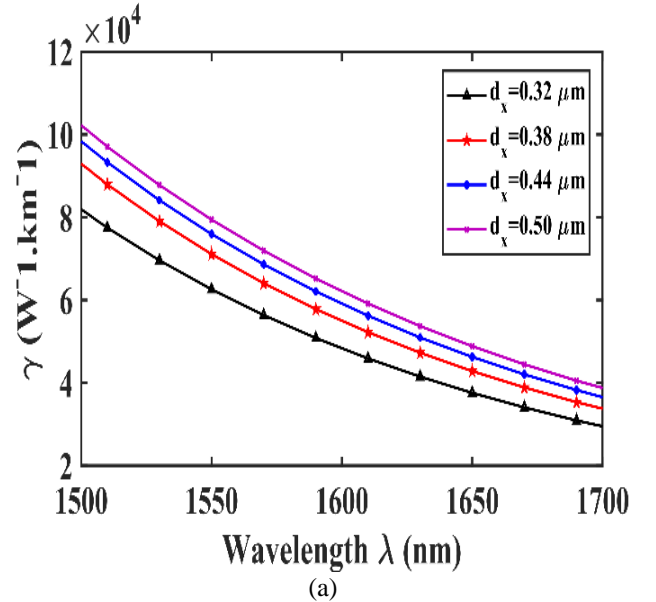
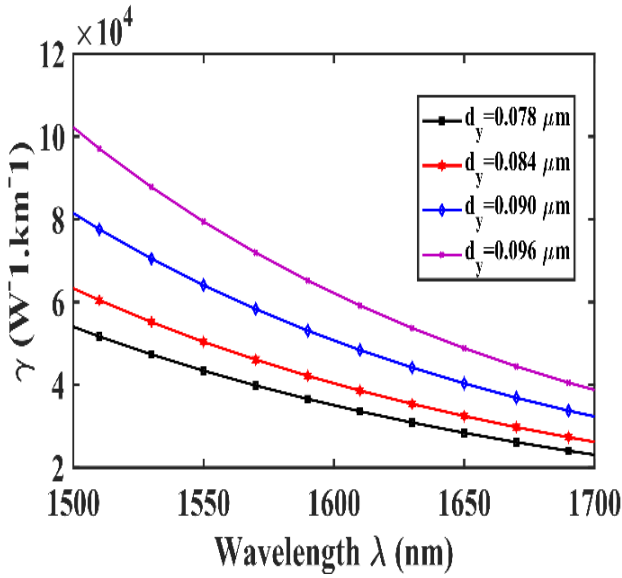


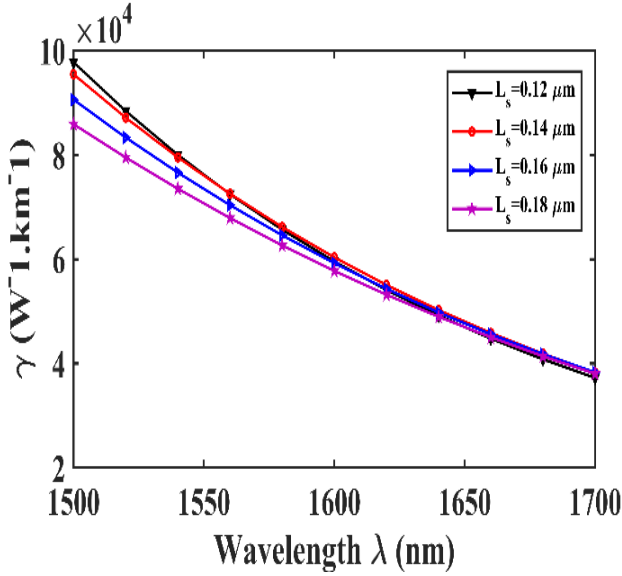
Fig. 3 Effective area of the proposed HNL-PCF as a function of wavelength with parameters $\Lambda = 0.75 \mu\text{m}$, $d = 0.58 \mu\text{m}$, $d_x = 0.5 \mu\text{m}$, $d_y = 0.096 \mu\text{m}$ and $L_s = 0.12 \mu\text{m}$.

Fig. 4 (a) shows the effect of variation in length of GaP strip on nonlinearity. It is apparent that increasing strip length d_x results in decreasing nonlinearity from 1500 nm to 1700 nm. At 1500 nm, nonlinearity is up to $10 \times 10^4 \text{ W}^{-1} \text{km}^{-1}$ whereas it would be up to $4 \times 10^4 \text{ W}^{-1} \text{km}^{-1}$ at 1700 nm wavelength. Similar effects are observed for increasing strip width d_y in Fig. 4 (b). For lower strip width, HNL-PCF has higher nonlinearity. This is because, by decreasing the strip length or width improves the light confinement in HNL-PCF which reduces the effective area and enhances the nonlinear coefficient.





(b)



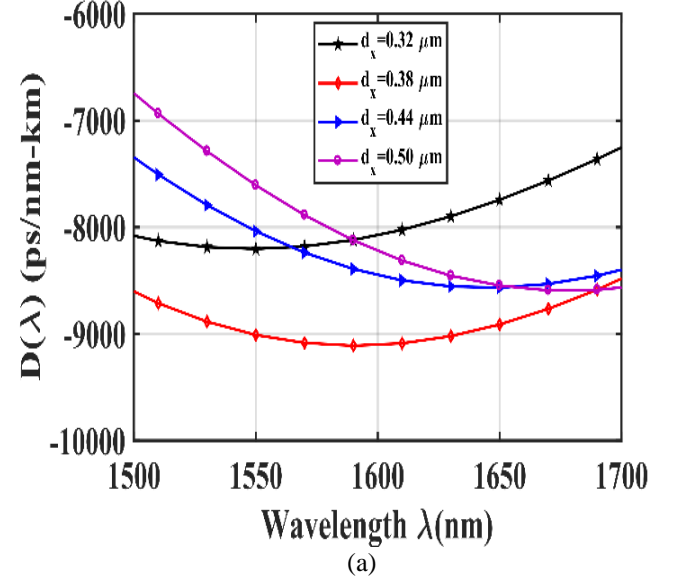
(c)

Fig. 4 Nonlinearity as a function of wavelength for variation of (a) strip length d_x , with $d_y = 0.096 \mu\text{m}$, $L_s = 0.12 \mu\text{m}$, $\Lambda = 0.75 \mu\text{m}$ and $d = 0.58 \mu\text{m}$; (b) strip width d_y , with $d_x = 0.50 \mu\text{m}$, $L_s = 0.12 \mu\text{m}$, $\Lambda = 0.75 \mu\text{m}$ and $d = 0.58 \mu\text{m}$ and (c) slot width L_s , with $d_x = 0.50 \mu\text{m}$, $d_y = 0.096 \mu\text{m}$, $L_s = 0.12 \mu\text{m}$, $\Lambda = 0.75 \mu\text{m}$ and $d = 0.58 \mu\text{m}$.

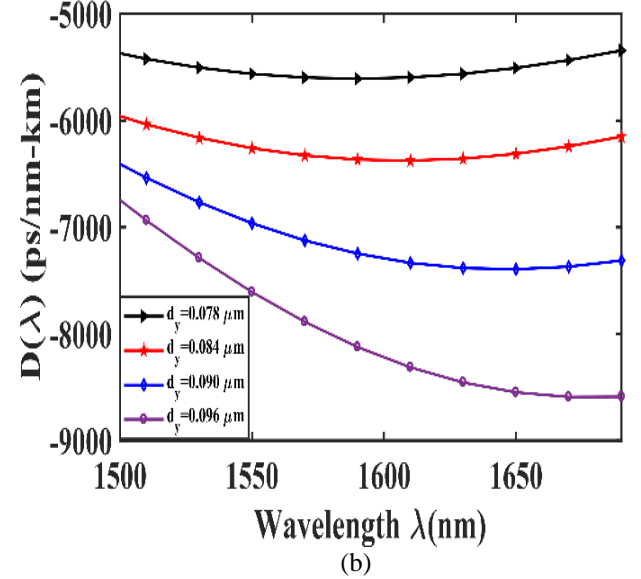
Fig. 4 (c) exhibits the effects of changing slot width on nonlinearity. It is clear that, increasing L_s reduces nonlinearity. At 1550 nm wavelength nonlinearity is $9.8 \times 10^4 \text{ W}^{-1}\text{km}^{-1}$ when $L_s = 0.12 \mu\text{m}$. However when $L_s = 0.18$, nonlinear coefficient reduces to $8.4 \times 10^4 \text{ W}^{-1}\text{km}^{-1}$. Since the slot width effective area increases, results in subsequent decrease in nonlinearity.

Chromatic dispersion of the proposed HNL-PCF is demonstrated in Fig 5(a), 5(b) and 5(c) by altering the parameters of d_x , d_y and L_s , respectively. In Fig 5(a), chromatic dispersion decreases with the increment of strip length d_x . At the communication band dispersion reaches up to $-9000 \text{ ps}/(\text{nm}\cdot\text{km})$. In Fig 5(b), strip width d_y is altered to see the effect of it. With the increment of strip width d_y , chromatic dispersion also increases and reaches up to $-7500 \text{ ps}/(\text{nm}\cdot\text{km})$ at 1550 nm wavelength. The effect of slot width L_s is explored in Fig. 5(c). From Fig. 5(c), it is clear that with the maximum slot width, we obtain the less dispersion. When the slot width $L_s = 0.12 \mu\text{m}$,

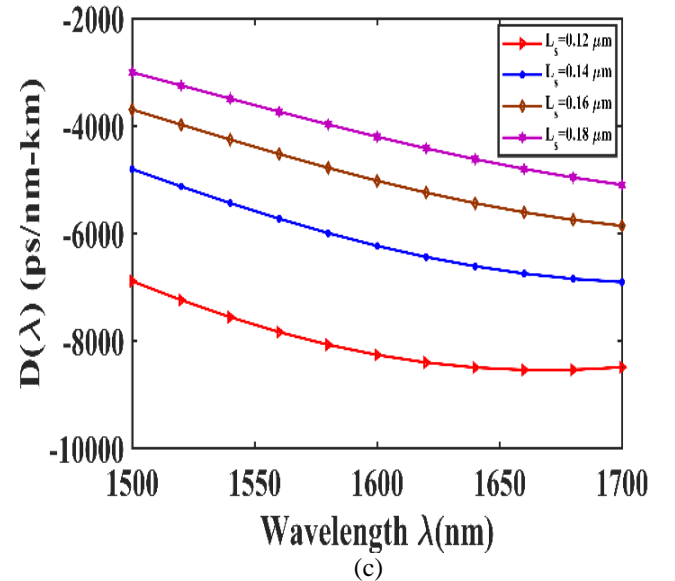
we acquire maximum dispersion of $-8000 \text{ ps}/(\text{nm}\cdot\text{km})$ at 1550 nm communication band.



(a)



(b)



(c)

Fig. 5 Chromatic dispersion as a function of wavelength for variation of (a) strip length d_x , with $d_y = 0.096 \mu\text{m}$, $L_s = 0.12 \mu\text{m}$, $\Lambda = 0.75 \mu\text{m}$ and $d = 0.58 \mu\text{m}$; (b) strip width d_y , with $d_x = 0.50 \mu\text{m}$, $L_s = 0.12 \mu\text{m}$, $\Lambda = 0.75 \mu\text{m}$ and $d = 0.58 \mu\text{m}$ and (c) slot width L_s , with $d_x = 0.50 \mu\text{m}$, $d_y = 0.096 \mu\text{m}$, $L_s = 0.12 \mu\text{m}$, $\Lambda = 0.75 \mu\text{m}$ and $d = 0.58 \mu\text{m}$.

Confinement loss of the suggested HNL-PCF is depicted in Fig 6. In Fig 6(a), strip length of GaP is varied keeping other parameters constant. With the increment of strip length d_x , confinement loss decreases. Similar effect is shown for the increment of strip width d_y . In both, case confinement loss can be as low as 10^{-3} dB/km. However, slot width has opposite effect. With the slot width L_s , confinement loss increases.

In simulation, we varied the slot width L_s , strip length d_x and strip width d_y keeping other parameters unaltered; i.e., pitch $\Lambda = 0.75 \mu\text{m}$ and diameter of air hole $d = 0.58 \mu\text{m}$ due to core length and width provided major effect on nonlinearity than cladding. Moreover, chromatic dispersion of the suggested HNL-PCF mainly depends on the L_x , d_x and d_y and these are justified by varying the core diameter which has less effect than strip width, length and slot width.

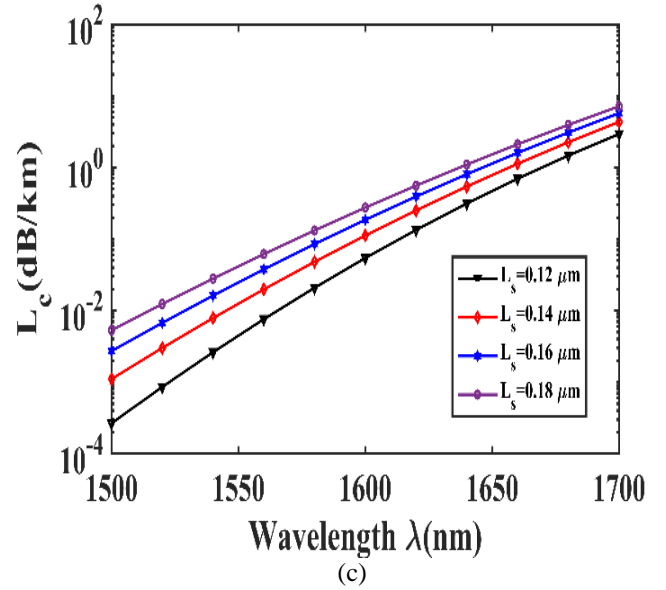
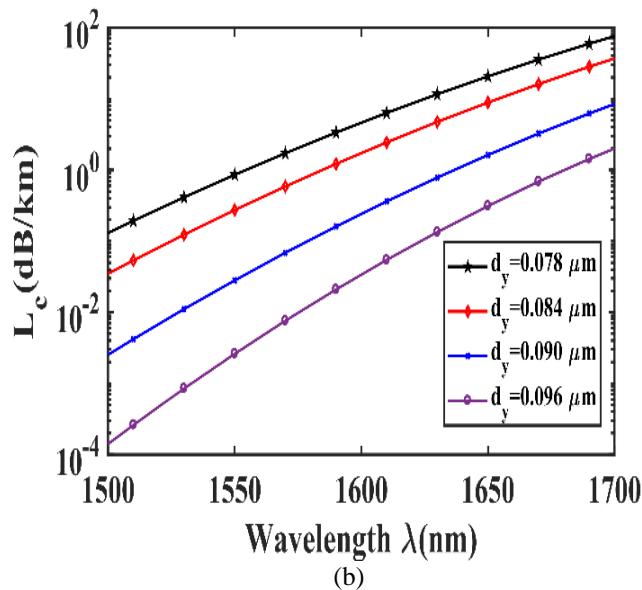
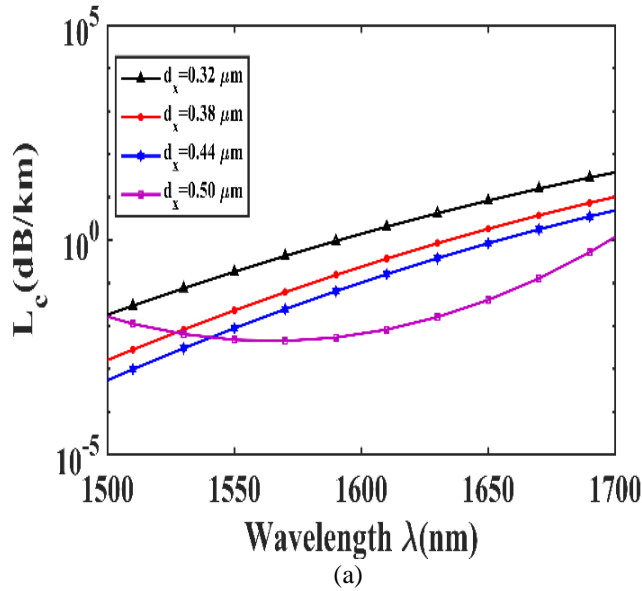


Fig. 6 Confinement loss as a function of wavelength for variation of (a) strip length d_x , with $d_y = 0.096 \mu\text{m}$, $L_s = 0.12 \mu\text{m}$, $\Lambda = 0.75 \mu\text{m}$ and $d = 0.58 \mu\text{m}$; (b) strip width d_y , with $d_x = 0.50 \mu\text{m}$, $L_s = 0.12 \mu\text{m}$, $\Lambda = 0.75 \mu\text{m}$ and $d = 0.58 \mu\text{m}$ and (c) slot width L_s , with $d_x = 0.50 \mu\text{m}$, $d_y = 0.096 \mu\text{m}$, $L_s = 0.12 \mu\text{m}$, $\Lambda = 0.75 \mu\text{m}$ and $d = 0.58 \mu\text{m}$.

IV. CONCLUSION

In this paper, we numerically investigated different optical properties of a HNL-PCF. The proposed HNL-PCF shows a very high nonlinearity up to $10 \times 10^4 \text{ W}^{-1} \text{ km}^{-1}$ and a very low confinement loss of 10^{-3} dB/km at 1550 nm wavelength. The fiber can have potential application in supercontinuum generation, optical parameter amplification and broadband dispersion compensation. To our best knowledge, nonlinearity that HNL-PCF shows is the highest compared to recently published articles.

REFERENCES

- [1] A. Wang *et al.*, "Visible Supercontinuum Generation With Sub-Nanosecond 532-nm Pulses in All-Solid Photonic Bandgap Fiber," *IEEE Photonics Technol. Lett.*, vol. 24, no. 2, pp. 143–145, Jan. 2012.
- [2] Y. P. Yatsenko and A. D. Pryamikov, "Parametric frequency conversion in photonic crystal fibres with germanosilicate core," *J. Opt. A Pure Appl. Opt.*, vol. 9, no. 7, pp. 716–722, Jul. 2007.
- [3] "Highly nonlinear photonic crystal fiber with ultrahigh birefringence using a nano-scale slot core," *Opt. Fiber Technol.*, vol. 22, pp. 107–112, Mar. 2015.
- [4] T. Huang, J. Liao, S. Fu, M. Tang, P. Shum, and D. Liu, "Slot Spiral Silicon Photonic Crystal Fiber With Property of Both High Birefringence and High Nonlinearity," *IEEE Photonics J.*, vol. 6, no. 3, pp. 1–7, Jun. 2014.
- [5] P. Li and J. Zhao, "Polarization-dependent coupling in gold-filled dual-core photonic crystal fibers," *Opt. Express*, vol. 21, no. 5, p. 5232, Mar. 2013.
- [6] J. Liao, J. Sun, M. Du, and Y. Qin, "Highly Nonlinear Dispersion-Flattened Slotted Spiral Photonic Crystal Fibers," *IEEE Photonics Technol. Lett.*, vol. 26, no. 4, pp. 380–383, Feb. 2014.
- [7] M. N. Amin and M. Faisal, "Highly nonlinear polarization-maintaining photonic crystal fiber with nanoscale GaP strips," *Appl. Opt.*, vol. 55, no. 35, p. 10030, Dec. 2016.

- [8] J. Hou, D. Bird, A. George, S. Maier, B. Kuhlmeier, and J. C. Knight, "Metallic mode confinement in microstructured fibres," *Opt. Express*, vol. 16, no. 9, p. 5983, Apr. 2008.
- [9] S. Selleri, L. Vincetti, A. Cucinotta, and M. Zoboli, "Complex FEM modal solver of optical waveguides with PML boundary conditions," *Opt. Quantum Electron.*, vol. 33, no. 4/5, pp. 359–371, 2001.
- [10] F. Liu *et al.*, "Three-photon absorption and Kerr nonlinearity in undoped bulk GaP excited by a femtosecond laser at 1040 nm," *J. Opt.*, vol. 12, no. 9, p. 95201, Sep. 2010.